Lost electron energy distribution of electron cyclotron resonance ion sources

I. Izotov, V. Skalyga, and O. Tarvainen

Published version information

Citation: I Izotov, V Skalyga and O Tarvainen. Lost electron energy distribution of electron cyclotron resonance ion sources. Rev Sci Instrum 93, no. 4 (2022): 043501

DOI: 10.1063/5.0075464

Lost electron energy distribution of electron cyclotron resonance ion sources

Cite as: Rev. Sci. Instrum. **93**, 043501 (2022); https://doi.org/10.1063/5.0075464
Submitted: 15 October 2021 • Accepted: 12 March 2022 • Published Online: 01 April 2022

I. Izotov, V. Skalyga and O. Tarvainen

Review of Scientific Instruments ARTICLE scitation.org/journal/rsi

Lost electron energy distribution of electron cyclotron resonance ion sources

Cite as: Rev. Sci. Instrum. 93, 043501 (2022); doi: 10.1063/5.0075464
Submitted: 15 October 2021 • Accepted: 12 March 2022 •
Published Online: 1 April 2022

I. Izotov,[1,2,a)] V. Skalyga,[1,2] and O. Tarvainen[3]

AFFILIATIONS

[1] Federal Research Center "Institute of Applied Physics of Russian Academy of Sciences," 603950 Nizhny Novgorod, Russia
[2] Lobachevsky State University of Nizhny Novgorod, 603950 Nizhny Novgorod, Russia
[3] STFC, ISIS Pulsed Spallation Neutron and Muon Facility, Rutherford Appleton Laboratory, Harwell OX11 0QX, United Kingdom

Note: This paper is a part of the Special Topic Collection on Ion Source Diagnostics.
[a)] **Author to whom correspondence should be addressed:** ivizot@ipfran.ru

ABSTRACT

To ensure further progress in the development of electron cyclotron resonance ion sources (ECRISs), deeper understanding of the underlying physics is required. The electron energy distribution (EED), which is crucial for the performance of an ECRIS, still remains obscure. The present paper focuses on the details of a well-developed technique of measuring the EED of electrons escaping axially from the magnetically confined plasma of an ECRIS. The method allows for better than 500 eV energy resolution over a range of electron energies from 4 keV to over 1 MeV. We present detailed explanation of the experimental procedure and the following data processing peculiarities with examples and discuss possible reasons of energetic electron losses from the magnetic trap, in particular the role of RF pitch angle scattering. Finally, an experimental method of approximating the confined EED based on the measurement of escaping electrons is described.

I. INTRODUCTION

Electron cyclotron resonance ion sources, pioneered by Geller[1] and Herbert and Wiesemann,[2] are widely used in accelerator-based nuclear physics research and applications owing to their capability to produce high charge state ions from a large number of elements. Furthermore, these versatile plasma ion sources produce ion beams of not only stable but also radioactive elements and intense beams of light ions, e.g., hydrogen and helium. A characteristic feature of the electron heating in the ECRIS plasma is that the electrons gain mostly (unless they are highly relativistic) transverse energy when interacting with the microwave electric field,[3–5] resulting in the electron velocity distribution (EVD) being strongly anisotropic. The electron energy distribution (EED) defines volumetric reaction rates and, most importantly, ionization and affects the growth and damping rates of nonlinear processes present in ECRIS plasmas. In particular, it has been shown that ECRIS plasmas are prone to kinetic instabilities stemming from the anisotropy of the EVD and non-equilibrium EED. The inevitable outcome of such instabilities is the periodic oscillation of the extracted ion beam current as a consequence to the loss of the ion confinement at each instability onset.[6]

Direct measurement of the EED in ECRIS plasmas is virtually impossible as all invasive diagnostic methods would disturb the system. Based on indirect measurements, reported, e.g., by Melin *et al.*[7] and Barue *et al.*,[8] the EED can be argued to consist of three main components: cold electrons with an average energy $\langle \varepsilon_{e,cold} \rangle$ of 10–100 eV, i.e., on the order of the plasma potential; warm electrons with $\langle \varepsilon_{e,warm} \rangle$ of 1–10 keV (most relevant for high charge state ionization); and hot electrons with $\langle \varepsilon_{e,hot} \rangle$ from 10 keV up to 1 MeV. In reality, the functional shape of the EED is likely more complex. Thus, further knowledge on the EED and, more importantly, the ability to control it through the operational parameters of the ion source are crucial for optimization of ECRIS performance and bench-marking particle-in-cell (PIC) simulation codes.

In the rarefied (i.e., microwave-transparent) plasma, both the acceleration of electrons produced in ionization of the neutral gas and their scattering rate to the loss cone (i.e., RF-scattering[3,4,9]) are determined by the electron–wave interaction. When electrons interact with a monochromatic electromagnetic wave in the ECR region, they are heated stochastically until their energy is high enough to render the difference between the wave and particle motion phases deterministic.[10] This leads to the collapse of the

Fermi acceleration regime, which implies that the electron energies are limited to a certain upper bound value, the EED forms a "quasilinear plateau"[3,4,10] in the resonance region of the momentum space, and the ability of the plasma to absorb the microwave energy is limited to the density growth only, while the shape of the EED remains unchanged. Such conditions are usually met at the initial breakdown stage of the ECR discharge, which explains some observations, e.g., the high microwave reflection associated with the plasma ignition[11] and the preglow effect.[12–14] When collisions are introduced at higher plasma density and/or the wave is not strictly monochromatic, the plateau-like EED collapses partially as the phase of the electron–wave interaction remains random for a certain fraction of the electrons, which enables their "overheating" up to MeV energies witnessed through a Bremsstrahlung diagnostic (e.g., paper by Gammino *et al.*[15]). Furthermore, collisions and collision-like processes alter the electron diffusion lines in momentum space and, thus, affect the EED through complex interactions. The resulting energy distribution has a sophisticated strongly non-Maxwellian shape, which prohibits invasive diagnostics and complicates indirect diagnostics of the EED due to deconvolution problems.

Information on the average energy of the cold electron population of an ECRIS can be attained through optical emission spectroscopy, as described by Kronholm *et al.*[16,17] The method is based on the comparison of the measured emission line intensities from two or more electronic states being populated by electron impact excitation from the same lower energy state (most often the ground state). The observed emission intensities can be connected to the $\langle \varepsilon_{e,cold} \rangle$-dependent rate coefficients, calculated from the known cross sections, assuming a certain EED, e.g., Maxwellian or Druyvesteyn, yielding values of 30–60 eV. Unfortunately, the line ratio method in the visible light emission range is not suitable for the detection of the warm or hot electron EED due to diminishing excitation cross sections to emitting states at higher electron energies.

When collisions are introduced at higher plasma density and/or the wave is not strictly monochromatic, the plateau-like EED partly collapses since the phase of electron–wave interaction remains random for a part of electrons, which enables "overheating" of the latter up to MeV energies as often detected through the Bremsstrahlung diagnostic (e.g., paper by Gammino *et al.*[15]). Furthermore, collisions and collision-like processes alter the electron diffusion lines in momentum space and, thus, affect the EEDF through complex interactions. The resulting energy distribution has a sophisticated shape, being strongly non-Maxwellian, which prohibits invasive diagnostics and complicates indirect diagnostics of the EED.

The parametric dependencies of the warm electron population can be measured through the detection of characteristic x-ray emission of a noble gas plasma.[18] The method could be improved by measuring the characteristic x-ray emission of multiple species simultaneously, which would, in principle, provide rudimentary information on the warm electron EED similar to the ratio of escaping and confined warm electron as described elsewhere.[19] Furthermore, characteristic x-ray emission (and plasma bremsstrahlung) can be detected with spatially resolving CCD-camera to obtain the distribution of warm electrons in the ECRIS plasma.[20]

Although it could be argued that the electrons with energies on the order of hundreds of keV play a minor role in ionization (which is the most relevant process for the application of an ECRIS) due to a small electron impact ionization cross section at relativistic energies, their energy distribution is still of great interest from practical and fundamental plasma physics point of view. In particular, high-energy electrons are considered to be responsible for the onset of cyclotron instabilities, which are widely recognized as a factor limiting the ECRIS performance.[6,22] Accumulation and losses of such energetic electrons are relevant for the local structure of the plasma potential and are believed to influence the overall plasma confinement, including electrostatic trapping of the high charge state ions.[22] Therefore, investigation of a high-energy tail of EEDF is considered to be of fundamental interest.

The above-mentioned characterization of a high energy part of the EED, based on plasma Bremsstrahlung spectroscopy, is a fairly simple and widely used method of tuning the ion source operational parameters (see, e.g., the paper by Benitez *et al.*[23] and references therein). However, the technique does not allow for unambiguous reconstruction of the EED, as the deconvolution is often compromised by the geometry of experiment and requires certain assumptions on the EEDF shape.[24] Plasma bremsstrahlung spectroscopy is therefore mostly used for estimation of a qualitative indicator of the plasma energy content, i.e., "spectral temperature," and the maximum energy of electrons. Unfortunately, the spectral temperature has little value for precise analysis of EED and nonlinear plasma–wave interactions. However, recent developments in spatially resolved plasma x-ray imaging[25] and self-consistent numerical modeling of ECRIS plasma[26] resulted in a very promising technique of evaluating the EED by a trial-and-error fitting method[27] in the 2–20 keV range, being the most influential on the highly charged ions formation.

Evidently, the EED can be measured directly, though in quite a narrow energy range. One of the simplest methods is Langmuir probe diagnostics and subsequent analysis of the I–V characteristics within the frame of Druyvesteyn theory.[28] However, even the modified Arslanbekov's theory, being successful for measuring the EED in low-temperature microwave-heated plasmas[29] of singly charged ions, is inapplicable for ECRIS of multicharged ions. This is due to the invasive nature of the probe, which in the case of rarefied ECRIS plasma perturbs the equilibrium and distorts the EED both locally and globally. Furthermore, the Langmuir probe technique is inapplicable for measuring electron energies in the keV–MeV range, especially in strong and spatially varying magnetic fields.

The present work focuses on the details of yet another fairly new method of EED evaluation based on the direct measurement of lost electron energy distribution (LEED), i.e., the energy distribution of electrons escaping the magnetic confinement axially, in the range of 4–1000 keV. We describe in detail all the peculiarities of the method, review the most recent examples of measurements, and discuss the possible correlation between the EED of confined and axially escaping electrons.

II. LEED MEASUREMENT TECHNIQUE

The essence of measuring electrons lost axially from the magnetic confinement (reasons of such losses are discussed further) through the magnetic mirror is to employ the bending magnet, which is normally present in the vast majority of ECR (and other) ion sources for m/q-separation of the extracted ion beams. With its

polarity reversed, electrons are allowed to travel along the path of the beamline, whereas positive particles are deflected toward the vacuum chamber walls. At the given field strength of the magnet, B, the apparatus deflects electrons with relativistic momentum $p = \gamma m_0 V = R|e|B$, where γ is the Lorentz factor, m_0 is the electron rest mass, V is the transverse speed of electrons, R is the curvature radius of particle trajectories inside the bending magnet, and $|e|$ is the elementary charge. Then, $\gamma = \sqrt{1 + \left(\frac{p}{m_0 c}\right)^2}$, and the electron kinetic energy is given as

$$\varepsilon = m_0 c^2(\gamma - 1) = m_0 c^2\left(\sqrt{1 + \left(\frac{R|e|B}{m_0 c}\right)^2} - 1\right), \quad (1)$$

where c is the speed of light (all units in SI).

Nominally, not only electrons but also negative ions may pass through the apparatus, whether the B-field strength matches its m/q ratio. For example, the H^- ion with 1 eV energy would have the same bending radius as the electron with an energy of 2 keV. However, negative ions may be easily filtered in the vicinity of the particle (current) detector.

In our experiments, the electrons escaping the magnetic confinement were detected with a secondary electron amplifier placed in the beamline downstream from the bending magnet used as an energy dispersive separator, as described above. To achieve good energy resolution, it is essential to collimate the electron flux. Normally, two 5 mm collimators placed between the ion source and the bending magnet and yet another 5 mm entrance collimator in front of the current detector were used. The plasma electrode itself also acts as a collimator. The use of the secondary electron amplifier as a current sensor yields two benefits: (a) current gain may be as high as 10^5 and (b) the amplifier cathode is biased with −4 kV usually, which ensures the apparatus detects only electrons, as the existence of negative ions with energies above 4 keV is highly unlikely. The drawback is inherently related to the latter benefit, i.e., the apparatus cannot detect electrons with energies below the (absolute value of the) bias potential. Most LEED measurements were performed at the 14 GHz ECR ion source,[30] located at the Jyvaskyla University, Finland. A schematic view of the experimental setup is shown in Fig. 1.

For the precise measurement of electron energy, the magnetic field deflecting the electrons should be measured with a calibrated high-resolution Hall-probe. It is possible to perform the measurements without the probe by estimating the bending field value out of the magnet current and its known geometry. However, this may lead to poor energy resolution. Furthermore, the hysteresis of the bending magnet yoke material would affect the measurement.

The power supply used for operating the bending magnet coil must have a high precision and small current step. Analog type power supply is highly preferable, enabling continuous ramp of the current. The plasma chamber of the ion source and all focusing electrodes should be grounded throughout the experiment. This ensures that the detected electron flux consists of the electrons leaking from the plasma through the extraction aperture retarded only by the plasma potential, which usually is in the range of several volts—several tens of volts.[31] It is worth noting that experiments with a biased plasma chamber seem to be possible, given that the transport function (explained further) is precisely calculated with all electric fields considered.

III. DATA PROCESSING

The data processing of the measured raw signals is a crucial step, as the shape of the measured LEED is strongly affected by several factors. The most fundamental one is the probability $P(\varepsilon)$ of reaching the detector for an electron with certain energy, referred to as "transport function" hereinafter. In the case of a conventional ECRIS, such as the JYFL 14 GHz ECRIS, and with all active beam optics (solenoids and xy-correction magnets) turned off and grounded (einzel lenses), the magnetic field downstream the plasma electrode is decreasing monotonically, and the transport function would normally be close to $P(\varepsilon) \sim \varepsilon$. This result was numerically obtained by means of particle tracking, assuming that the electron distribution at the extraction aperture is independent of energy and has a KV-distribution.[32] In the case of more complex trap field and beamline optics, the transport function may become sophisticated.

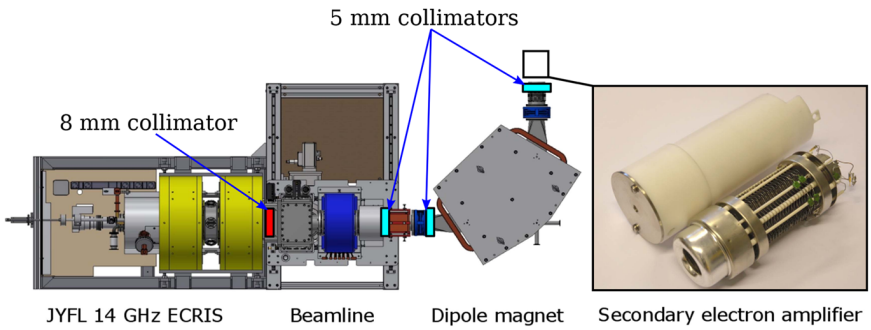

FIG. 1. A schematic view of the experimental setup (left) and a photograph of the secondary electron amplifier (right). The JYFL 14 GHz ECRIS has an 8 mm plasma electrode aperture, and the low energy beamline is equipped with 5 mm collimators placed between the solenoid (blue) and the 90° dipole magnet, which is used as an electron spectrometer. The secondary electron amplifier is placed at the end of the displayed beamline section. In the photograph, the insulating cover (white) and d = 5 mm entrance collimator of the amplifier have been removed and placed to the background to reveal the amplifier chain.

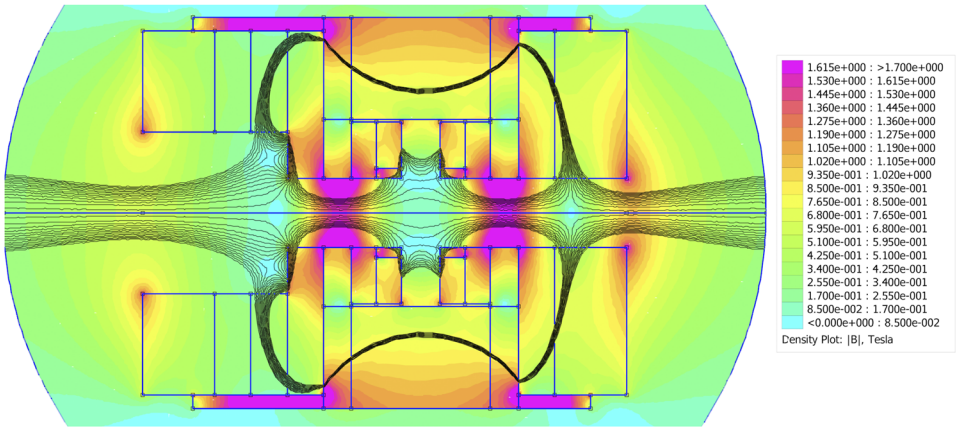

FIG. 2. Magnetic field distribution at the GISMO facility. The extraction region is on the left.

For example, at the GISMO (Gasdynamic Ion Source for Multi-purpose Operation) facility,[33] which is a gasdynamic high current ECRIS at IAP RAS, Nizhny Novgorod, Russia, the magnetic trap is all a permanent magnet. This leads to variations of the magnetic field in the extraction and beam propagation region. The magnetic field heat map of the GISMO facility is shown in Fig. 2. The zero-field area in the beamline and the adjacent downstream field maximum greatly affect the transport function, making it non-monotonic. In the case of GISMO, the transport function was also simulated with a particle tracking code. As an example, the transport function (assuming initial KV distribution) is shown in Fig. 3 for both JYFL and GISMO facilities.

The influence of the transport function on the post-processed LEED is shown in Fig. 4, where an example of the measured LEED is plotted with and without the correction applied as $f(\varepsilon)_{corrected} = f(\varepsilon)_{raw}/P(\varepsilon)$.

Besides the electron transport, the current sensor may have its own peculiarities. The secondary electron amplifier (see Fig. 1) functions by emitting secondary electrons from the biased aluminum cathode and amplifying the signal by a chain of subsequent meshes (dynodes) before measuring the current from the grounded anode. The energy dependent yield of the secondary electrons[34] released from the amplifier cathode must be taken into account during the data analysis. The electron backscattering coefficient[35] also slightly affects measurements.

We have established two common procedures for LEED measurement, i.e., "continuous scan" and "pulsed scan." The former one is applicable for a stable operation mode of the ion source, whereas the latter one is suitable in circumstances where the plasma parameters are changing rapidly, e.g., in the unstable mode. The continuous scan, as the phrase implies, utilizes slow ramping of the bending magnet current and, thus, the magnetic field. Both the magnetic field and the electron current are measured simultaneously, yielding an I_e vs B plot. Then, the B-field value is converted to electron energy according to Eq. (1). The energy resolution of such a scan is determined, besides the electron optics, by the current measurement scheme self-capacitance and inductance compared to the ramp speed. In our experiments, we succeeded to achieve a resolution

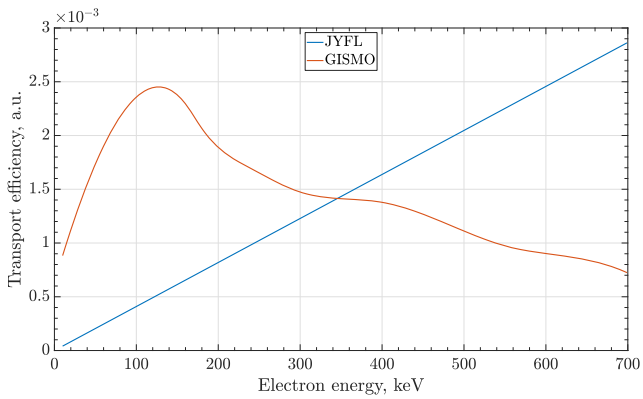

FIG. 3. Electron transport efficiency vs electron energy.

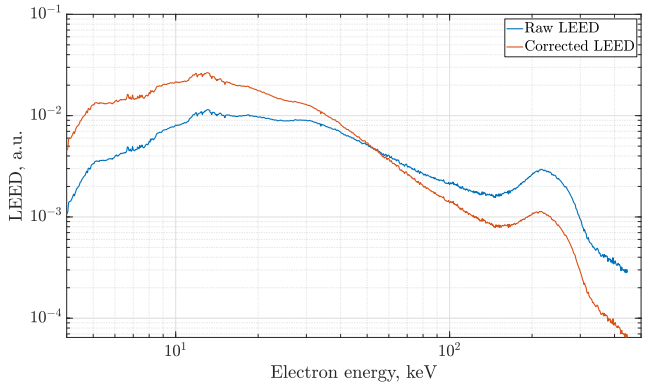

FIG. 4. An example of the measured LEED with and without the transport function applied. The data were obtained at the JYFL ECRIS facility.

better than 500 eV,[30] i.e., $\Delta E/E$ of better than 0.005 for 100 keV electrons, which is the relevant order of magnitude here. The aforementioned resolution was estimated by means of the same particle tracking procedure used for transport function evaluation, and the result of 0.005 is the FWHM (full width at half maximum) of the (numerically) "detected" peak while (numerically) "ramping" the bending magnet field, whereas initial particles had the energy of 100 keV and K–V phase space distribution at the plasma electrode. The energy resolution may be improved even more by reducing collimators diameter; however, this would naturally lead to the degradation of the signal. Therefore, higher gain would be required. The real energy resolution might be also measured by extracting electrons from the plasma with known energy; however, the extraction voltage must be much higher than plasma potential, i.e., on the order of several tens of kV to achieve a reliable result. This has been done recently at the GISMO facility, and the experiment confirmed numerical estimation of the energy resolution.

The other procedure, i.e., "pulsed scan," is applicable when the time-resolved LEED is of interest. In this case, the measurement should be triggered by an event of some sort, e.g., the onset of a kinetic instability or the leading edge of the microwave heating pulse. Then, the measurement is performed during a pre-established time span, within which the bending field value remains constant. After the single acquisition is finished (and often averaged over multiple triggers), the bending field value is changed, and the system is initialized for the next trigger event. The described procedure allows us to construct a 3D plot of LEED dynamics. It is of note that for the "pulsed" scan mode, the reproducibility of all signals must be high in order to obtain fine details; otherwise, the LEED fine details would be blurred. In our experiments, we kept the source parameters in the range where kinetic instabilities are not very pronounced, thus ensuring excellent signal reproducibility.

The example of data from the "continuous scan" is shown in Fig. 4, and the example of data from the "pulsed" scan is shown in Fig. 5. A distinct feature of the LEED is the high energy hump at 150–300 keV, which we discuss in detail below.

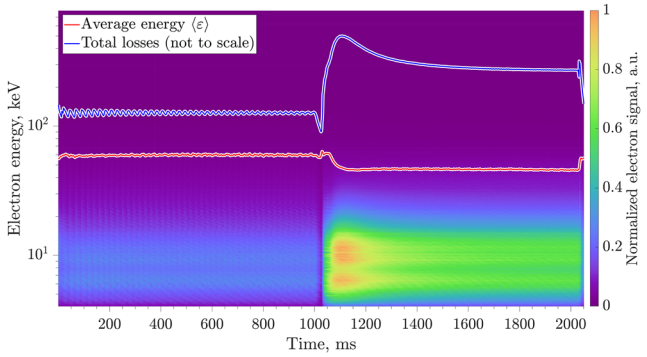

FIG. 5. Example of the LEED measured in the "pulsed mode," showing the transition between unstable and stable plasmas. Source settings: single frequency heating at 12 GHz, 15 W (1000 ms)/50 W (1000 ms), $B_{min}/B_{ECR} = 0.98$, $3.5 \cdot 10^{-7}$ mbar oxygen pressure. A microwave pulse was used as a trigger source. The data were taken at JYFL ECRIS.

IV. QUASILINEAR DIFFUSION AND RF-SCATTERING

The electron transverse and longitudinal momentum is increased in the resonant interaction between an electron and the microwave electromagnetic field.[3,4] The increment of the longitudinal momentum change increases with the electron energy, causing high energy electrons to diffuse to the loss cone in the momentum space, thus exiting the magnetic trap in a process called "RF scattering." This model allows for a qualitative explanation for high energy electron losses. Unfortunately, even the relativistic model cannot explain all features of the experimentally observed LEED,[3,4,9,30,36] i.e., the energy distribution of the electrons escaping the trap through the magnetic mirror covers a wide range of energies. In contrast, the simplified relativistic model[3,4] predicts that electrons escape with a fixed energy determined by the ratio between the microwave frequency and the electron cyclotron frequency at the mirror point. This result follows from the simplifying assumptions of the model stating that the plane electromagnetic wave interacting with the electrons propagates along the magnetic field and has a relatively weak amplitude and small vacuum wave number. In reality, the energy distribution of the escaping electrons can be affected by collisions, disturbances, and attenuation of the incident electromagnetic wave and the fact that the heating wave is never strictly monochromatic. Recent experiments have revealed that the RF-scattering contributes significantly to electron losses in the range of 20–570 keV.[36,37] The measurement of the LEED allows for characterizing the EED inside the trap, but the relative importance of this mechanism for total electron losses and the energy dependence of its efficiency remain elusive.

To find an alternative mechanism to explain the wide energy dispersion of LEED, we discuss the evolution of the electron distribution function within a quasi-linear theory.[38–40] Our application of the aforementioned theory to an open magnetic trap follows the considered methodology described in Refs. 41 and 42.

The quasi-linear approximation is plausible when electrons need many passes through the ECR zone to obtain significant energy, and there is no phase correlation between subsequent passes (in an open trap, it also implies that the bounce oscillation time of the electron is much longer than the time of one pass of the ECR zone). For a conventional ECR ion source, these assumptions are usually valid. Then, in the interaction of a monochromatic wave with a collisionless electron, the following value is an invariant:

$$\mathcal{K} = \varepsilon - \omega J_\perp = \text{const}, \tag{2}$$

where ε is the kinetic energy of the electron and $J_\perp = m_e\gamma^2 v_\perp^2/2\omega_B(z)$ is the transverse adiabatic invariant. Here, we assume that electrons confined in the magnetic trap are bouncing along magnetic field lines, and their longitudinal and perpendicular velocities change so that γ and $J_\perp$ remain constant; $\omega_B(z)$ denotes the change in the gyrofrequency along the magnetic field line. $\mathcal{K}$ = const are quasi-linear diffusion lines in momentum space. The cyclotron interaction reduces to an alignment of the electron distribution function along these lines. Such a process is usually limited either by the entry of the particle into a loss cone or by reaching values of energy and adiabatic invariant at which the ECR condition is no longer satisfied anywhere in the inhomogeneous magnetic field. Another possible mechanism of limitation of quasilinear diffusion is the so-called superadiabatic

effect,[10] which we do not consider because stationary plasma density in the ECR ion source is believed to be too high for the effect to exist.

A confined electron bounces along the magnetic field between two mirror points where $v_\parallel = 0$. Conservation of $J_\perp$ and γ or, equivalently, of $v_\perp^2/\omega_B$ and $v_\perp^2 + v_\parallel^2$ allows us to determine the value of the gyrofrequency ω_B^* at the mirror point as

$$\omega_B^*(J_\perp, \gamma) = \frac{v_\perp^2 + v_\parallel^2}{v_\perp^2} \quad \omega_B(z) = \frac{(\gamma^2 - 1)\, m_e c^2}{2 J_\perp}. \tag{3}$$

Thus, for the particle with a given $(J_\perp, \gamma)$, the range of magnetic field magnitude would be

$$\omega_B^{\min} \le \omega_B(z) \le \omega_B^*(J_\perp, \gamma), \tag{4}$$

where $\omega_B^{\min}$ is the minimum gyrofrequency at the center of the trap. The ECR condition at the fundamental harmonic (1) can be reformulated as

$$\omega_B^{\text{res}}/\omega - \gamma = \pm n_\parallel \sqrt{(\gamma^2 - 1)(1 - \omega_B^{\text{res}}/\omega_B^*)}. \tag{5}$$

Because of the strong slowing down of right-hand polarized waves near the cold resonance, i.e., $n_\parallel \gg 1$ for $\omega_B \approx \omega$, condition (5) is fulfilled for any electron that can reach the "cold" ECR $\omega_B = \omega$ during its movement along the magnetic field line. Compared with (4), it is found to be possible when

$$\omega_B^{\min} < \omega \le \omega_B^*(J_\perp, \gamma). \tag{6}$$

This condition is valid if the following holds:

- The plasma is not too rarefied, $\omega_p^2/\omega_B^2 \gtrsim \sqrt{T_e/m_e c^2}$, with T_e being the characteristic temperature of the bulk electrons so that the whistler-like dispersion relation is valid (this condition is fulfilled in reported experiments).
- The heating frequency is higher than the minimum gyrofrequency in the trap.
- The heating electric field is non-zero in the entire volume of the plasma, rather than being focused into a spot.

Then, condition (6) ensures that an electron with a given $(J_\perp, \gamma)$ meets the real "hot" cyclotron resonance somewhere along the magnetic field line.

A similar condition can be written for the entry of an electron into a loss cone, characterized by the maximum value of the magnetic field along the field line,

$$\omega_B^{\max} \le \omega_B^*(J_\perp, \gamma), \tag{7}$$

where $\omega_B^{\max}$ is the maximum value of gyrofrequency achieved in the magnetic mirror. This condition enables a simple physical interpretation: when the turning point ω_B^* corresponds to the value of the magnetic field above the maximum one along the trajectory, the electron is able to leave the trap (the ambipolar potential is much less than kinetic energies considered here).

It is convenient to introduce a new variable,

$$\kappa \equiv \omega_B^{\min}/\omega_B^* \propto J_\perp/(\gamma^2 - 1), \tag{8}$$

and use it instead of $J_\perp$. Physically, $\kappa = \sin^2\vartheta$, where ϑ is the angle between the electron velocity and the magnetic field at the center of the trap; therefore, $\kappa = 0$ and $\kappa = 1$ correspond, respectively, to electrons moving freely along the B-field without cyclotron gyration and gyrating in the B-field minimum without longitudinal motion. Then, conditions (6) and (7) are translated to simple vertical boundaries in (κ, γ)-space: $\kappa \le \omega_B^{\min}/\omega$ for the ECR presence (6) and $\kappa \le \omega_B^{\min}/\omega_B^{\max}$ for the loss cone (7). To summarize, in a sufficiently dense plasma, effective heating and confinement are possible when

$$\omega_B^{\min}/\omega_B^{\max} \le \kappa \le \omega_B^{\min}/\omega < 1, \tag{9}$$

and this condition is independent of the kinetic energy of the electron γ.

An example of diffusion lines is shown in Fig. 6 in (κ, γ)-space. The group of diffusion curves for the 14 GHz and $B_{\min} = 0.372$ T and $B_{\max} = B_{\text{ext}} = 0.908$ T (typical JYFL operation mode) is shown in black. The κ range defined in (9) for these parameters is $0.41 < \kappa \le 0.74$. The diffusion curves differ only in the value of $\mathscr{K}$ in (2), which effectively are different initial conditions (spread of velocities) for accelerated electrons. A quasi-one-dimensional distribution function localized along the $\mathscr{K} = 0$ curve, shown in a bold black line, is formed from electrons with initially low energy. This diffusion asymptote lies entirely in the region where the inequality (6) is true and intersects the loss cone at

$$\gamma^* = 2\omega_B^{\max}/\omega - 1. \tag{10}$$

This equation follows from (2) with $\mathscr{K} = 0$ and (3) at the boundary of the loss-cone $\omega_B^* = \omega_B^{\max}$, i.e., $\gamma - 1 = \omega J_\perp/m_e c^2$ and $\gamma^2 - 1 = 2\omega_B^{\max} J_\perp/m_e c^2$. Following calculations above and very similar to the simplified model,[3,4] LEED should consist of a sharp and pronounced peak with central energy at $\gamma^* = 2\omega_B^{\max}/\omega - 1$ (which gives $\varepsilon = 736$ keV for nominal experimental conditions at JYFL ion source) with some background signal arising from rare collisions and electrons, which are born in the loss-cone region. However, experimental observations strongly contradict this conclusion. Thus, the measured LEED cannot be explained exclusively by quasi-linear

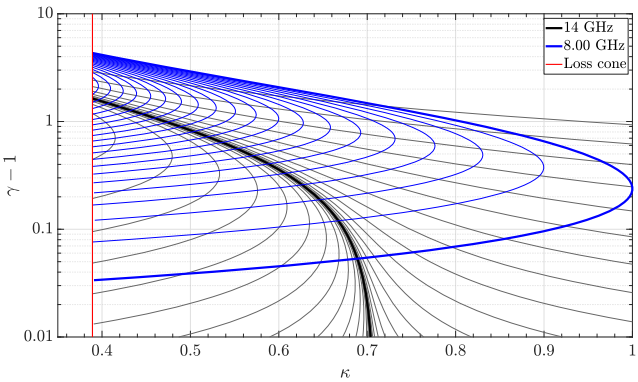

FIG. 6. The group of quasi-linear diffusion lines at 14 GHz (black) and 8 GHz (blue) and the loss cone (red) calculated for magnetic configuration: $B_{\min} = 0.372$ T, $B_{\max} = B_{\text{ext}} = 0.908$ T. The minimum and maximum cyclotron frequencies are, accordingly, 10.4 and 25.4 GHz.

diffusion resulting from the interaction with a monochromatic heating wave at 14 GHz.

In order to explain the experimental data, we have to develop a model. This idea together with detailed calculations was first proposed to explain the high energy hump often observed in LEED.[9] Suppose that there is a secondary electromagnetic wave with a frequency below the minimum cyclotron frequency. A non-resonant wave with $\omega < \omega_B^{\min}$ cannot be substantially slowed down by the plasma, so the dense plasma argument is inapplicable. The resonance condition (5) must be treated differently. Indeed, for constrained $n_\parallel$, there is a minimal energy of the electron at which interaction with the monochromatic wave is possible with a Doppler shift of the relativistic cyclotron resonance. When a secondary electromagnetic wave is excited, a quasi-one-dimensional distribution function propagates along diffusion curves corresponding to an extra frequency (shown in blue in Fig. 6). In this case, there are two mechanisms of electron loss: first, direct diffusion along blue curves in interaction with the second frequency and second, diffusion along blue curves can "carry" particles to black diffusion curves corresponding to the main heating frequency, and these diffusion lines can then lead to a loss cone. Thus, addition of a secondary frequency not only introduces extra losses of energetic electrons but also transforms a quasi-one-dimensional distribution function into fully two-dimensional one. Depending on the frequency ω_{II} of the secondary wave, additional electron losses can be introduced over the whole range of energies when $\omega_{\text{II}} > \omega_B^{\min}$ or when $\omega_{\text{II}} < \omega_B^{\min}$, be more pronounced only at energies above some threshold γ_l, defined as the point where the diffusion line tangent to $\kappa = 1$ intersects the loss cone $\kappa = \omega_B^{\min}/\omega_B^{\max}$.

The above approach explains some features of the LEED shape and its dependence on parameters,[9] although the origin of the secondary electromagnetic wave remains unclear. According to the experimental data, this supposed wave is switched on and off together with the heating radiation, although its frequency is independent of the primary heating frequency. The simplest explanation seems to be a plasma-filled cavity mode, excited by a strongly heated unstable plasma inside, but this requires experimental verification, presenting a clear need for diagnostics.

V. RECONSTRUCTION OF THE EED

Regardless of the processes responsible for the loss of energetic electrons from the magnetic trap, there appears to be a straightforward technique to reconstruct or at least approximate the EED by measuring the LEED in the aforementioned "pulsed" mode. The technique is based on the following approach. First, plasma is allowed to reach a steady-state and then the microwave radiation is switched off, and the current of the electrons escaping through the extraction mirror during the plasma decay is measured. Thus, the following dataset is obtained:

$$I_e = I_e(t, \varepsilon), \tag{11}$$

where $I_e(t)$ is the waveform of electron current at a fixed bending magnetic field or, the same, electron energy ε.

The microwave pulse duration must ensure a saturation of relevant plasma parameters. The best way to determine the minimum pulse duration, in our opinion, would be to measure the ion beam spectrum with different pulse lengths and then define the pulse duration at which the average ion charge saturates. The saturation of the ion charge state distribution very likely means the saturation of EED and plasma density. The total recorded time period for each heating pulse should be long enough to ensure that the electron signal dissipates during the plasma decay.

In the absence of RF pitch angle scattering (and afterglow instabilities), collisional scattering is the main process pushing electrons into the loss cone. Assuming that the majority of the collisions are elastic (the validity of such assumption needs further investigations) and not changing the electron energy, electron losses integrated over the plasma decay can be argued to represent the information on the EED prevailing inside the plasma at the moment when the microwaves are switched off,

$$f(\varepsilon) = \frac{\int_{t_1}^{t_2} I_e(t, \varepsilon)\, dt}{\int_{t_1}^{t_2} \int_{\varepsilon_1}^{\varepsilon_2} I_e(t, \varepsilon)\, dt\, d\varepsilon}, \tag{12}$$

where t_1 and t_2 are the microwave pulse trailing edge and the time when the electron signal reaches zero, respectively, and ε_1 and ε_2 are the lower and upper limit of the measured electron energies.

An example of such evaluation acquired at JYFL 14 GHz ECRIS is represented in Fig. 7 (red curve) together with LEED measured before the trailing edge of the heating pulse (blue curve). Both curves are normalized to the unity square, i.e., they are the distribution functions. The source settings were the following: single-frequency heating at 14 GHz with 260 W, pulse length: 624 ms, and repetition rate: 1 Hz; $B_{\min}/B_{ECR} = 0.73$, $3.5 \cdot 10^{-7}$ mbar oxygen pressure.

The two distributions are similar. The main difference is the absence of the high-energy hump in the reconstructed EED (which complies with the presumable origin of the hump being RF-scattering[9]) and a more gentle slope of the reconstructed EED in the energy range of 20–200 keV when compared to the LEED. It is of note that the method might be affected by afterglow instabilities, which are inevitably developing during the plasma decay.[43] More experimental studies and, most likely, a comparison to PIC simulations are required to further confirm the validity of the proposed method.

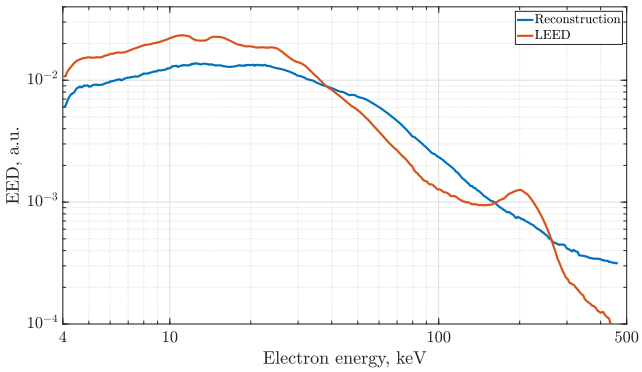

FIG. 7. Comparison of the LEED and EED reconstructed from the plasma decay. Source settings: single-frequency heating at 14 GHz, 260 W, $B_{\min}/B_{ECR} = 0.73$, and oxygen pressure: $3.5 \cdot 10^{-7}$ mbar. The data were taken at JYFL 14 GHz ECRIS.

VI. CONCLUSION

All the LEEDs we have detected thus far have a linear (high energy) tail on logarithmic scale, which must not be mistakenly associated with a Maxwellian EED: A linear fit yields too high electron temperature for the fitting region, implying that a Maxwellian fit is inapplicable. This emphasizes the fact that the LEED and, therefore, the EED are strictly non-Maxwellian. The described technique of the LEED measurement yields information on the process of the EED formation in the ECR-heated plasma confined in any type of the open magnetic system. We are actively pursuing to develop methods to precisely and unambiguously deconvolute the energy distribution of lost electrons back to the energy distribution of the confined electrons. These methods are based on the Fokker–Planck equation being solved within the balanced model of step-wise ionization. Additional measurements of the LEED with different ECR ion sources are needed for bench-marking the deconvolution procedure, especially the experiments with modern super-conducting sources operating at a higher frequency/stronger magnetic field.

The described experimental procedure has obvious advantages over Bremsstrahlung diagnostics in terms of estimating the efficiency of ECR heating and electron confinement in modern ECRISs. That is because the outcome of the LEED measurement is not the qualitative "spectral temperature," but rather a fine structure of the energy distribution (of lost electrons). Unfortunately, it is impossible to measure the LEED and the ion beam parameters simultaneously in contrast to Bremsstrahlung. However, as the described method is non-invasive, unlike Langmuir probe diagnostics, it is possible to correlate plasma and/or ion beam parameters (measured separately) with the EED. We have observed that the LEED measured with the ion source grounded is different from the LEED with the source potential applied, which underlines the importance of conducting ECRIS plasma diagnostic experiments under ion source relevant conditions, i.e., with the source potential switched on. Finally, we note that the direct measurement of electron energies is of obvious interest for fundamental research in the field of ECR heating and for open mirror fusion machines, not just ion sources.

ACKNOWLEDGMENTS

This work was supported by the Russian Science Foundation under Project Grant No. 19-12-00377.

AUTHOR DECLARATIONS

Conflict of Interest

The authors have no conflicts to disclose.

DATA AVAILABILITY

The data that support the findings of this study are available from the corresponding author upon reasonable request.

REFERENCES

[1]R. Geller, "Electron cyclotron resonance multiply charged ion sources," IEEE Trans. Nucl. Sci. **23**(2), 904 (1972).
[2]K. C. Herbert and K. Wiesemann, "Production of highly charged ions in plasmas with high electron temperature (in german)," GSI-Bericht **71**, 171 (1971).
[3]V. A. Zhiltsov, A. A. Skovoroda, A. V. Timofeev, K. Y. Kharitonov, and A. G. Sherbakov, Fiz. Plasmy **17**, 771 (1991).
[4]V. A. Zhiltsov, Y. A. Kuyanov, A. A. Skovoroda, and A. V. Timofeev, Fiz. Plasmy **20**, 267 (1994).
[5]A. Girard, C. Perret, G. Melin, and C. Lécot, "Modeling of electron-cyclotron-resonance ion source and scaling laws," Rev. Sci. Instrum. **69**, 1100 (1998).
[6]O. Tarvainen, I. Izotov, D. Mansfeld, V. Skalyga, S. Golubev, T. Kalvas, H. Koivisto, J. Komppula, R. Kronholm, J. Laulainen, and V. Toivanen, "Beam current oscillations driven by cyclotron instabilities in a minimum-B confined electron cyclotron resonance ion source plasma," Plasma Sources Sci. Technol. **23**, 025020 (2014).
[7]G. Melin, F. Bourg, P. Briand, J. Debernardi, M. Delaunay, R. Geller, B. Jacquot, P. Ludwig, T. K. N'Guyen, L. Pin, M. Pontonnier, J. C. Rocco, and F. Zadworny, "Some particular aspects of the physics of the ECR sources for multicharged ions," Rev. Sci. Instrum. **61**, 236–238 (1990).
[8]C. Barué, M. Lamoureux, P. Briand, A. Girard, and G. Melin, "Investigation of hot electrons in electron-cyclotron-resonance ion sources," J. Appl. Phys. **76**, 2662–2670 (1994).
[9]I. V. Izotov, A. G. Shalashov, V. A. Skalyga, E. D. Gospodchikov, O. Tarvainen, V. E. Mironov, H. Koivisto, R. Kronholm, V. Toivanen, and B. Bhaskar, "The role of radio frequency scattering in high-energy electron losses from minimum-B ECR ion source," Plasma Phys. Controlled Fusion **63**, 045007 (2021).
[10]E. V. Suvorov and M. D. Tokman, Sov. J. Plasma Phys. **15**, 540 (1989).
[11]T. Ropponen, O. Tarvainen, I. Izotov, J. Noland, V. Toivanen, G. Machicoane, D. Leitner, H. Koivisto, T. Kalvas, P. Peura, P. Jones, V. Skalyga, and V. Zorin, "Studies of plasma breakdown and electron heating on a 14 GHz ECR ion source through measurement of plasma bremsstrahlung," Plasma Sources Sci. Technol. **20**, 055007 (2011).
[12]I. V. Izotov, A. V. Sidorov, V. A. Skalyga, V. G. Zorin, T. Lamy, L. Latrasse, and T. Thuillier, "Experimental and theoretical investigation of the Preglow in ECRIS," IEEE Trans. Plasma Sci. **36**, 1494–1501 (2008).
[13]T. Thuillier, T. Lamy, L. Latrasse, I. V. Izotov, A. V. Sidorov, V. A. Skalyga, V. G. Zorin, and M. Marie-Jeanne, "Study of pulsed electron cyclotron resonance ion source plasma near breakdown: The preglow," Rev. Sci. Instrum. **79**, 02A314 (2008).
[14]V. Skalyga, I. Izotov, V. Zorin, and A. Sidorov, "Physical principles of the preglow effect and scaling of its basic parameters for electron cyclotron resonance sources of multicharged ions," Phys. Plasmas **19**, 023509 (2012).
[15]S. Gammino, D. Mascali, L. Celona, F. Maimone, and G. Ciavola, "Considerations on the role of the magnetic field gradient in ECR ion sources and build-up of hot electron component," Plasma Sources Sci. Technol. **18**, 045016 (2009).
[16]R. Kronholm, T. Kalvas, H. Koivisto, and O. Tarvainen, "Spectroscopic method to study low charge state ion and cold electron population in ECRIS plasma," Rev. Sci. Instrum. **89**, 043506 (2018).
[17]R. Kronholm, T. Kalvas, H. Koivisto, S. Kosonen, M. Marttinen, D. Neben, M. Sakildien, O. Tarvainen, and V. Toivanen, "ECRIS plasma spectroscopy with a high resolution spectrometer," Rev. Sci. Instrum. **91**, 013318 (2020).
[18]M. Sakildien, R. Kronholm, O. Tarvainen, T. Kalvas, P. Jones, R. Thomae, and H. Koivisto, "Inner shell ionization of argon in ECRIS plasma," Nucl. Instrum. Methods Phys. Res., Sect. A **900**, 40–52 (2018).
[19]M. Sakildien, O. Tarvainen, R. Kronholm, I. Izotov, V. Skalyga, T. Kalvas, P. Jones, and H. Koivisto, "Experimental evidence on microwave induced electron losses from ECRIS plasma," Phys. Plasmas **25**, 062502 (2018).
[20]R. Rácz, D. Mascali, S. Biri, C. Caliri, G. Castro, A. Galatà, S. Gammino, L. Neri, J. Pálinkás, F. P. Romano, and G. Torrisi, "Electron cyclotron resonance ion source plasma characterization by energy dispersive X-ray imaging," Plasma Sources Sci. Technol. **26**, 075011 (2017).
[21]O. Tarvainen, J. Laulainen, J. Komppula, R. Kronholm, T. Kalvas, H. Koivisto, I. Izotov, D. Mansfeld, and V. Skalyga, "Limitations of electron cyclotron resonance ion source performances set by kinetic plasma instabilities," Rev. Sci. Instrum. **86**, 023301 (2015).
[22]V. P. Pastukhov, Rev. Plasma Phys. **13**, 203 (1987).
[23]J. Benitez, C. Lyneis, L. Phair, D. Todd, and D. Xie, "Dependence of the bremsstrahlung spectral temperature in minimum-B electron cyclotron resonance ion sources," IEEE Trans. Plasma Sci. **45**, 1746–1754 (2017).

[24]S. Kasthurirangan, A. N. Agnihotri, C. A. Desai, and L. C. Tribedi, "Temperature diagnostics of ECR plasma by measurement of electron bremsstrahlung," Rev. Sci. Instrum. **83**, 073111 (2012).
[25]S. Biri, R. Rácz, Z. Perduk, J. Pálinkás, E. Naselli, M. Mazzaglia, G. Torrisi, G. Castro, L. Celona, S. Gammino, A. Galatá, F. P. Romano, C. Caliri, and D. Mascali, "Innovative experimental setup for X-ray imaging to study energetic magnetized plasmas," J. Instrum. **16**, P03003 (2021).
[26]C. S. Gallo, A. Galatà, G. Torrisi, and D. Mascali, "Self-consistent electromagnetic analysis of the microwave-coupling of an electron cyclotron resonance-based charge breeder," Rev. Sci. Instrum. **91**, 033501 (2020).
[27]B. Mishra, A. Pidatella, S. Biri, A. Galatà, E. Naselli, R. Rácz, G. Torrisi, and D. Mascali, "A novel numerical tool to study electron energy distribution functions of spatially-anisotropic and non-homogeneous ECR plasmas," arXiv:2107.01457 [physics.plasm-ph] (2021).
[28]M. J. Druyvesteyn, "Der niedervoltbogen," Z. Phys. **64**, 781–798 (1930).
[29]J. L. Jauberteau, I. Jauberteau, O. D. Cortázar, and A. Megía-Macías, "Time evolution of the electron energy distribution function in pulsed microwave magnetoplasma in H_2," Phys. Plasmas **23**, 033513 (2016).
[30]I. Izotov, O. Tarvainen, V. Skalyga, D. Mansfeld, T. Kalvas, H. Koivisto, and R. Kronholm, "Measurement of the energy distribution of electrons escaping minimum-B ECR plasmas," Plasma Sources Sci. Technol. **27**, 025012 (2018).
[31]O. Tarvainen, P. Suominen, T. Ropponen, T. Kalvas, P. Heikkinen, and H. Koivisto, "Effect of the gas mixing technique on the plasma potential and emittance of the JYFL 14 GHz electron cyclotron resonance ion source," Rev. Sci. Instrum. **76**, 093304 (2005).
[32]V. Toivanen, T. Kalvas, H. Koivisto, J. Komppula, and O. Tarvainen, "Double einzel lens extraction for the JYFL 14 GHz ECR ion source designed with IBSimu," J. Instrum. **8**, P05003 (2013).
[33]V. A. Skalyga, A. F. Bokhanov, S. V. Golubev, I. V. Izotov, M. Y. Kazakov, E. M. Kiseleva, R. L. Lapin, S. V. Razin, R. A. Shaposhnikov, and S. S. Vybin, "Status of the gasdynamic ion source for multipurpose operation (GISMO) development at IAP RAS," Rev. Sci. Instrum. **90**, 123308 (2019).
[34]Y. Lin and D. C. Joy, "A new examination of secondary electron yield data," Surf. Interface Anal. **37**, 895–900 (2005).
[35]T. Tabata, "Backscattering coefficients of electrons: A review," in Proceedings of the Fourteenth EGS Users' Meeting in Japan (published online 2007).
[36]S. V. Golubev, I. V. Izotov, D. A. Mansfeld, and V. E. Semenov, "Experimental electron energy distribution function investigation at initial stage of electron cyclotron resonance discharge," Rev. Sci. Instrum. **83**, 02B504 (2012).
[37]I. Izotov, D. Mansfeld, V. Skalyga, V. Zorin, T. Grahn, T. Kalvas, H. Koivisto, J. Komppula, P. Peura, O. Tarvainen, and V. Toivanen, "Plasma instability in the afterglow of electron cyclotron resonance discharge sustained in a mirror trap," Phys. Plasmas **19**, 122501 (2012).
[38]M. E. Mauel, "Electron-cyclotron heating in a pulsed mirror experiment," Phys. Fluids **27**, 2899 (1984).
[39]H. L. Berk, "Derivation of the quasi-linear equation in a magnetic field," J. Plasma Phys. **20**, 205 (1978).
[40]I. B. Bernstein and D. C. Baxter, "Relativistic theory of electron cyclotron resonance heating," Phys. Fluids **24**, 108 (1981).
[41]A. G. Shalashov, E. D. Gospodchikov, and I. V. Izotov, "Electron-cyclotron heating and kinetic instabilities of a mirror-confined plasma: the quasilinear theory revised," Plasma Phys. Controlled Fusion **62**, 065005 (2020).
[42]A. G. Shalashov, E. D. Gospodchikov, and I. V. Izotov, "Addendum: Electron-cyclotron heating and kinetic instabilities of a mirror-confined plasma: the quasi-linear theory revised (2020 *Plasma Phys. Control. Fusion* 62 065005)," Plasma Phys. Controlled Fusion **62**, 119401 (2020).
[43]D. Mansfeld, I. Izotov, V. Skalyga, O. Tarvainen, T. Kalvas, H. Koivisto, J. Komppula, R. Kronholm, and J. Laulainen, "Dynamic regimes of cyclotron instability in the afterglow mode of minimum-B electron cyclotron resonance ion source plasma," Plasma Phys. Controlled Fusion **58**, 045019 (2016).